Tetrahedron: *Asymmetry* 20 (2009) 1027–1035

Contents lists available at ScienceDirect

Tetrahedron: *Asymmetry*

journal homepage: www.elsevier.com/locate/tetasy

Assignment of absolute configurations of permethrin and its synthon 3-(2,2-dichlorovinyl)-2,2-dimethylcyclopropanecarboxylic acid by electronic circular dichroism, optical rotation, and X-ray crystallography

Wolfgang Bicker [a,*], Karol Kacprzak [b,*], Marcin Kwit [b], Michael Lämmerhofer [a], Jacek Gawronski [b], Wolfgang Lindner [a]

[a] *Christian Doppler Laboratory for Molecular Recognition Materials, Department of Analytical Chemistry and Food Chemistry, University of Vienna, Waehringer Strasse 38, A-1090 Vienna, Austria*
[b] *Faculty of Chemistry, A. Mickiewicz University, ul. Grunwaldzka 6, PL-60780 Poznań, Poland*

ARTICLE INFO

Article history:
Received 7 January 2009
Accepted 11 March 2009
Available online 7 May 2009

ABSTRACT

The availability of single stereoisomers of biologically/toxicologically relevant chiral compounds such as the pyrethroid-type insecticide permethrin (PM) and the reliable determination of their absolute configurations are of central importance for the detailed investigation and correct assignment of stereoselective effects. In this context, single stereoisomers of 3-(2,2-dichlorovinyl)-2,2-dimethylcyclopropanecarboxylic acid (DCCA), a precursor, metabolite, and environmental degradation product of PM, were isolated from a mixture of all four stereoisomers in enantiomeric excesses of >99% via a two-step chromatographic process combining a diastereoselective reversed-phase separation in the first step with a direct enantiomer separation in the second step. Esterification of DCCA stereoisomers with 3-phenoxybenzyl alcohol yielded PM. Electronic circular dichroism (ECD) spectra of DCCA and PM stereoisomers were measured in non-polar (cyclohexane containing 5% v/v 1,2-dichloroethane) and non-protic polar (acetonitrile) solvents. Cotton effects suitable to distinguish the four stereoisomers of each DCCA and PM were obtained. Absolute configurations of DCCA were determined by confrontation of calculated (time-dependent density-functional theory using B3LYP hybrid functional) and experimental ECD and optical rotation (OR) data. Fully convergent results between ECD and X-ray diffractometry (analysis of DCCA isomers co-crystallized with *O*-9-(2,6-diisopropylphenylcarbamoyl)quinine), which was employed as a reference method, were obtained. The importance of considering dimer formation of DCCA in solution for the computational delineation of absolute configurations was demonstrated by (1*R*,3*R*)-*cis*-DCCA for which the ΔG Boltzmann averaged calculated monomeric form delivered the opposite sign of OR compared to the dimeric form and the value determined experimentally in dichloromethane. For (1*S*,3*R*)-*trans*-DCCA both monomer and dimer delivered the identical sign of OR and this was in agreement with the experimental measurement. In contrast to OR, the calculated ECD spectra of these two DCCA stereoisomers were less sensitive toward intermolecular association.

© 2009 Elsevier Ltd. All rights reserved.

1. Introduction

X-ray crystallography is a standard approach for the direct assignment of absolute configurations of chiral molecules but it is limited to the solid state.[1,2] Based on the substantial improvements in computing capacity and quantum-mechanical calculation methods, respectively, liquid state spectroscopic approaches such as electronic circular dichroism (ECD) and optical rotation (OR) have become increasingly popular alternatives to diffractometry especially when suitable crystals are difficult to be obtained.[3] The most straightforward and reliable approach to deduce information on absolute configurations from ECD or OR measurements is the confrontation of experimental (configuration not known) and theoretical (calculated for assumed configuration) data. This concept has been successfully applied for both configurational and conformational assignments for a variety of rigid as well as flexible molecules.[4–17] Although the detailed computational parameters are rather case sensitive, time-dependent density-functional theory (TDDFT) using B3LYP hybrid functional[18] in conjunction with enhanced basis sets (at least Aug-CC-pVDZ) is commonly used and provides a good compromise between accuracy and computational costs.

A proper conformational analysis of the target molecule is, however, a prerequisite for the reliability of this confrontation

* Corresponding authors. Tel.: +43 1 4277 52323; fax: +43 1 4277 9573 (W.B.); tel.: +48 61 8291367; fax: +48 61 8658008 (K.K).
E-mail addresses: wolfgang.bicker@univie.ac.at (W. Bicker), karol.kacprzak@gmail.com (K. Kacprzak).

0957-4166/$ - see front matter © 2009 Elsevier Ltd. All rights reserved.
doi:10.1016/j.tetasy.2009.03.035

approach. The utmost importance of this step lies in the fact that even minor changes in molecule conformation can result in a change of sign and/or magnitude of calculated ECD and OR data[9,19–26] thus bearing considerable risk for wrong assignments. This holds particularly true for conformationally labile compounds and therefore the relative energies of the participating conformers should be calculated with the highest available accuracy.[27–29] In addition to that, the potential occurrence of intermolecular associations has to be considered as well when computing ECD and OR data.[30]

The alkene-substituted cyclopropane ring system is a structural motif in many natural and synthetic compounds, including the natural pyrethrin-type insecticides and many of their synthetic pyrethroid analogues.[31] The non-substituted cyclopropane ring exhibits high HOMO energy whereas the LUMO energy is low. It is therefore an expectation that the cyclopropyl ring acts as both a good π donor and a good π acceptor[32] which in case of an alkene substituent undergoes hyperconjugation to a degree between a saturated and an unsaturated group. This has been demonstrated, for example, for the optically active dictyopterenes A and B.[33]

Systematic studies on the spectroscopic effects of cyclopropane-substituted alkenes have been published by Poulter.[34] Large bathochromic shifts of 8–15 nm for the π–π^* transition of the alkene chromophore due to hyperconjugation with the cyclopropyl ring were observed. Other authors[33,35–39] also suggested π–π^* transition as being a major contribution to electronic spectra of alkene-substituted cyclopropanes including pyrethrins[37] in the short-wavelength region.

In the field of ECD spectroscopy, studies suggested that the vinylcyclopropane motif is an inherently chiral chromophore, in which rotation of charge takes place along the bond connecting the three-membered ring with the double bond.[40,41] Thereby, the sign of the Cotton effect generated by this helically translated charge is the same as the sign of the acute angle between bisectrix and double bond.

In our ongoing work on the chemical[42,43] and biological properties[44] of pyrethroid stereoisomers and their (chiral) synthons and phase I metabolites, respectively, we became interested in characterizing the chiroptical properties of the pyrethroic acid 3-(2,2-dichlorovinyl)-2,2-dimethylcyclopropanecarboxylic acid (DCCA) **1**, ***ent*-1**, **2**, ***ent*-2** and permethrin (PM) **3**, ***ent*-3**, **4**, ***ent*-4**, particularly aiming at determination of the absolute configurations of their individual stereoisomers.

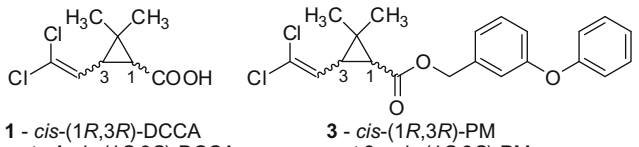

1 - *cis*-(1*R*,3*R*)-DCCA
***ent* - 1**-*cis*-(1*S*,3*S*)-DCCA
2 - *trans*-(1*R*,3*S*)-DCCA
***ent*-2** - *trans*-(1*S*,3*R*)-DCCA

3 - *cis*-(1*R*,3*R*)-PM
***ent*-3** - *cis*-(1*S*,3*S*)-PM
4 - *trans*-(1*R*,3*S*)-PM
***ent* - 4**-*trans*-(1*S*,3*R*)-PM

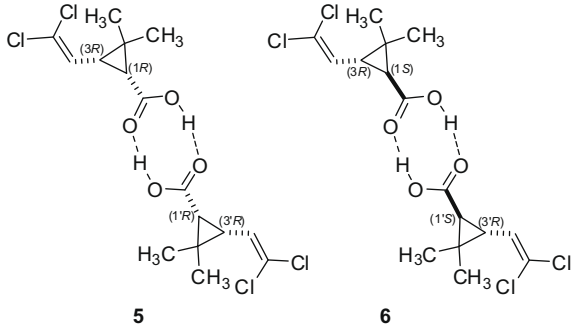

5 **6**

Due to the lack of commercial sources for the set of single stereoisomers of DCCA and PM, respectively, a two-step chromatographic method was developed to obtain all four single DCCA stereoisomers which were converted to the corresponding PM stereoisomers via a simple esterification step. Experimental ECD and OR data were used to determine absolute configurations via confrontation with calculated data. As independent method for verification of the correct assignment of absolute configurations, X-ray diffractometry data from single DCCA stereoisomers co-crystallized with *O*-9-(2,6-diisopropylphenylcarbamoyl)quinine were available from an earlier study.[42]

2. Results and discussion

2.1. Preparation of DCCA and PM stereoisomers

Previous work showed that cinchona-based chiral stationary phases exhibit stereorecognition capabilities for a variety of pyrethroic acids. This allows for their enantioselective but also diastereoselective separation by high-performance liquid chromatography (HPLC).[43]

Chiralpak QN-AX and Chiralpak QD-AX (Fig. 1), respectively, allowed baseline separation of all four DCCA stereoisomers in polar-organic mode under analytical conditions. However, at preparative scale either loading capacity or stereoisomeric purity had to be sacrificed and thus a two-step chromatographic separation was chosen to yield the individual stereoisomers of DCCA.

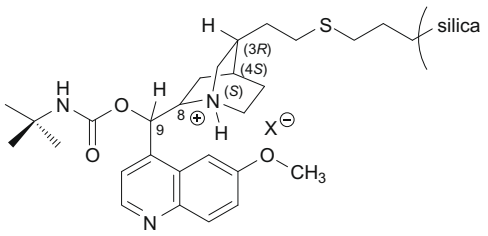

Figure 1. Structure of the chiral stationary phases based on *O*-9-(*tert*-butylcarbamoyl)quinine (8*S*,9*R*) (trade name: Chiralpak QN-AX) and quinidine (8*R*,9*S*) (trade name: Chiralpak QD-AX), respectively.

In a first step, diastereoselective separation of DCCA was achieved on a conventional C_{18} reversed-phase (RP) type stationary phase in preparative format injecting ca. 50 mg of the *cis*/*trans*-mixture of DCCA per run (Fig. 2a) (*Note*: *cis*/*trans* nomenclature refers to the spatial orientation of the C-3 dichlorovinyl substituent relative to the C-1 carboxylic acid at the cyclopropane ring of DCCA). The individual *cis*-DCCA and *trans*-DCCA diastereomers were then successfully resolved into the single enantiomers on Chiralpak QD-AX (Fig. 2b). Although higher mass loads would have been tolerated by the employed 250 × 20 mm ID Chiralpak QD-AX column, 50 mg of the racemate was injected per run, still yielding baseline resolution, in order to end up with high enantiomeric excess (ee).

The overall yield of DCCA stereoisomers after the dual chromatographic process was in the range of 80%. According to analytical RP-HPLC-UV diastereomeric purity was always better than 99% and no other chemical impurities were detected. Enantiomeric purity as determined with an analytical Chiralpak QN-AX column (showing reversed enantiomer elution order compared to the corresponding Chiralpak QD-AX column[43]), was between 99.2% and 99.9% ee for the various DCCA stereoisomers.

In a second step, stereoisomers of PM were synthesized from the stereoisomerically pure DCCA building blocks. Thus, DCCA isomers were reacted with oxalyl chloride to obtain the correspond-

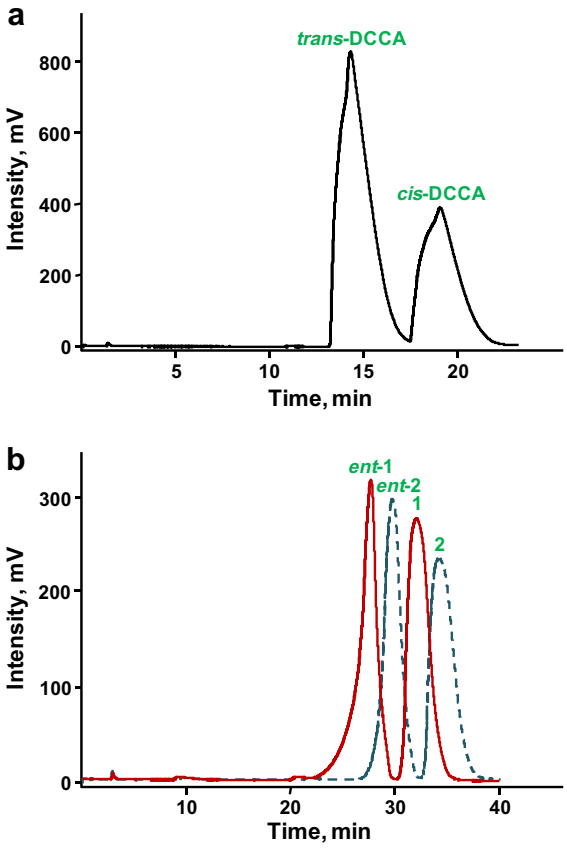

Figure 2. Preparative separation of (a) DCCA diastereomers on a Purospher Star RP-C18ec column and (b) *cis*-DCCA (red, solid line) and *trans*-DCCA (blue, dashed line) enantiomers, respectively, on a Chiralpak QD-AX column (overlay of two separate runs with the individual diastereomers). Chromatographic conditions are given in Section 4.

ing acid chlorides. These intermediates were then esterified with an excess of 3-phenoxybenzyl alcohol and were purified chromatographically by preparative RP-HPLC. The PM stereoisomers were obtained in 63–70% yield and the analytical control by RP-HPLC-UV showed that diastereomeric impurities amounted to less than 0.1%. Absence of racemization at either of the two chiral centers during synthesis was verified by quantitative hydrolysis of PM stereoisomers in alkaline medium and subsequent diastereoselective and enantioselective chromatography of the DCCA stereoisomers formed (Fig. 3).

2.2. Assignment of absolute configurations of DCCA by X-ray crystallography

X-ray diffractometry of co-crystals of all four DCCA stereoisomers with *O*-9-(2,6-diisopropylphenylcarbamoyl)quinine, a chiral selector previously found to exhibit higher enantioselectivity toward DCCA stereoisomers compared to *O*-9-(*tert*-butylcarbamoyl)quinine,[43] allowed the unequivocal assignment of absolute configurations for DCCA. In addition to that, the data gave valuable insight into the chiral recognition mechanism between this guest molecule and the chiral selector host. Detailed results of this comprehensive study, which besides X-ray crystallography consisted also of ^{1}H NMR and thermodynamic experiments as well as computational investigations, were subjects of a previous communication.[42] In the present work the X-ray data served as reference method for the determination of absolute configurations of DCCA by ECD and OR (vide infra).

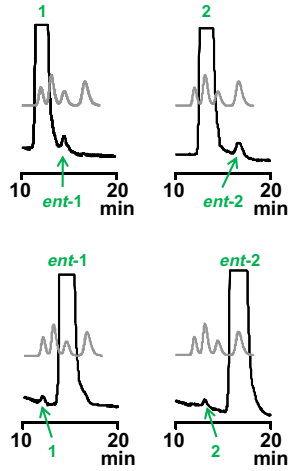

Figure 3. Enantiomeric purity of PM stereoisomers as determined by HPLC-UV analysis on Chiralpak QN-AX after alkaline hydrolysis to the corresponding DCCA stereoisomers. Diastereomeric purity of PM stereoisomers was independently checked by RP-HPLC-UV. Chromatograms in gray color show the reference separation of the DCCA stereoisomer mixture (*cis*/*trans*-ratio approximately 40:60). Chromatographic conditions are given in Section 4.

2.3. Assignment of absolute configurations of DCCA by ECD and OR data

2.3.1. Experimental determination

DCCA and PM contain a number of distinctly different chromophores. In case of DCCA these are the gem-disubstituted vinyl motif, the cyclopropane ring, and the carboxylic group. Both the carboxylic acid and the vinyl functionality are directly attached to the cyclopropane ring allowing their mutual electronic interactions. In the case of PM an additional aromatic moiety is present. Except the cyclopropane ring itself, in the selected wavelength range of 185–300 nm all these chromophores exhibit UV and consequently CD absorption in a similar spectral region which was thought to deliver complex UV and ECD spectra with overlapping transition bands. The experimental findings are summarized in Table 1.

UV spectra of *cis*-DCCA and *trans*-DCCA showed a high degree of similarity in the two selected solvent systems of contrasting polarity (acetonitrile; cyclohexane + 5% v/v 1,2-dichloroethane) with an absorption maximum around 215 nm. For PM the additional contribution from the 3-phenoxybenzyl chromophore was evident. Thereby, *cis*-PM enantiomers **3** and ***ent*-3** gave slightly lower molar absorption coefficients in short-wavelength region compared to *trans*-PM enantiomers **4** and ***ent*-4**.

In acetonitrile *cis*-DCCA enantiomer **1** showed a bisignate Cotton effect located at 213 nm ($\Delta\varepsilon = +13.2$) and at 187 nm ($\Delta\varepsilon = -10.6$). In cyclohexane only long-wavelength Cotton effects were observed due to the lower UV transparency of this solvent. The first one appeared at 242 nm with a small positive amplitude ($\Delta\varepsilon = +0.5$) while the second one had almost identical characteristics to those observed in acetonitrile and was located at 213 nm ($\Delta\varepsilon = +14.0$). The opposite *cis*-DCCA enantiomer ***ent*-1** showed similar locations of Cotton effects and these were in virtually perfect mirror–image relationships to **1** with regard to signs and amplitudes. This expected trend was also present for the second enantiomeric pair of DCCA and the two PM enantiomer pairs (vide infra).

trans-DCCA enantiomers **2** and ***ent*-2** delivered a weak long-wavelength Cotton effect at ca. 240 nm and a broadened short-wavelength transition at ca. 200 nm of lower amplitude in acetonitrile. In cyclohexane, the long-wavelength Cotton effect showed a hypsochromic shift by 7–9 nm and an almost fivefold increase of the amplitude whereas the short-wavelength band

Table 1
Experimental ECD and UV data for DCCA and PM stereoisomers

Compound	Acetonitrile		Cyclohexane[a]	
	ECD, $\Delta\varepsilon$ (nm)	ECD, $\Delta\varepsilon$ (nm)	ECD, $\Delta\varepsilon$ (nm)	UV, ε (nm)
1		12,000 (214)	+0.5 (242)	
	+13.2 (213)	8100 (186)	+14.0 (213)	11,600 (213)
	−10.6 (186)			
***ent*-1**			−0.5 (241)	
	−13.0 (213)		−14.2 (213)	
	+10.8 (187)			
2	−0.8 (238)	12,500 (213)	−3.9 (231)	12,000 (215)
	+6.6 (200)		+7.8 (205)	
***ent*-2**	+0.8 (241)		+4.0 (232)	
	−6.6 (201)		−7.6 (206)	
3		1900 (273)	−1.6 (230)	1800 (273)
		48,800 (197)	−1.9 (226)	15,000 (215)
	+10.7 (210)	52,000 (190)	+8.9 (209)	38,700 (205)
	−4.1 (189)			
***ent*-3**			+1.4 (232)	
			+1.7 (225)	
	−10.6 (210)		−8.6 (208)	
	+1.0 (188)			
4		1500 (278)	−0.2 (263)	1800 (273)
	−10.5 (222)	1600 (272)	−12.1 (222)	17,000 (230)
	+16.3 (197)	39,000 (203)	+8.7 (205)	43,600 (202)
		50,000 (189)		
***ent*-4**			+0.2 (262)	
	+8.8 (222)		+12.4 (221)	
	−13.9 (195)		−8.9 (205)	

[a] Containing 5% (v/v) 1,2-dichloroethane.

was bathochromically shifted by 5 nm accompanied by an increase in the amplitude by ca. 20%.

cis-PM enantiomer **3** delivered two Cotton effects of opposite sign in acetonitrile, one positive at 210 nm ($\Delta\varepsilon$ = +10.7) and one negative at 189 nm ($\Delta\varepsilon$ = −4.1). In cyclohexane, additional negative broad long-wavelength Cotton effects at ca. 230 nm were observed for **3**. This broad band showed at least two distinct maxima at 226 and 230 nm with amplitudes of −1.9 and −1.6, respectively. The major transition of **3** in cyclohexane, was similar to that in acetonitrile, located at 209 nm and also showed comparable amplitude ($\Delta\varepsilon$ = +8.9).

Opposed to the findings for **3**, *trans*-PM enantiomer **4** gave Cotton effects at 222 nm ($\Delta\varepsilon$ = −10.5) and 197 nm ($\Delta\varepsilon$ = +16.3) in acetonitrile. In cyclohexane Cotton effects at 222 nm ($\Delta\varepsilon$ = −12.1) and 205 nm ($\Delta\varepsilon$ = +8.7) as well as a small long-wavelength transition at 263 nm ($\Delta\varepsilon$ = −0.2) were observed.

This experimental series revealed that the enantiomeric forms of **1**–**4** can be easily differentiated with the aid of ECD spectroscopy. The esterification of DCCA with 3-phenoxybenzyl alcohol does not change the principal ECD properties of the resulting PM stereoisomers. Furthermore, the locations of major diagnostic Cotton effects as well as their signs and, in most cases, their amplitudes were not significantly influenced by the type of solvent and this held true for both DCCA and PM.

Due to the complex nature of the vinylcyclopropane chromophore the origins of the observed transitions are not entirely clear. Nevertheless, some general conclusions can be deduced. The short-wavelength absorption in UV and ECD spectra presumably originates from π–π^* transition of the dichlorovinylcyclopropane chromophore, although many other transitions of lower intensity may contribute to the absorption spectrum in this region as well. On the other hand, the small long-wavelength Cotton effects in the range of 230–240 nm, which were strongly affected by solvent polarity, may be assigned to n–π^* transitions in chlorine atoms. The long-wavelength band observed for **4** and ***ent*-4** in cyclohexane at 263 nm originates from the ^1L_b transition of the aromatic chromophore.

With respect to OR measurements all four DCCA stereoisomers gave specific OR values of about ±40° at the sodium D line (589.3 nm) in dichloromethane and they increased significantly when going to shorter wavelengths (Table 2).

Due to the presence of two stereogenic centers in DCCA it is evident that the sign of OR is an insufficient stereochemical descriptor to pinpoint the identity of the stereoisomers at least as long as no information on the diastereomeric type (*cis* or *trans*) is available.

2.3.2. Computational determination and confrontation with experimental data

In order to correlate experimental ECD spectra and OR data with absolute configurations extensive theoretical studies on structure–chiroptical properties relationships were performed for DCCA. The considerably higher structural complexity of PM did not allow us to carry out ab initio calculations within a reasonable timeframe. Absolute configurations of PM were, however, available as the synthesis route employed for PM was carried out under preservation of the absolute configurations of the single stereoisomer DCCA synthons.

Table 2
OR values calculated at the TDDFT/B3LYP/Aug-CC-pVDZ level for **1**, **5**, ***ent*-2**, and **6** and measured in dichloromethane for **1**, ***ent*-1**, **2**, and ***ent*-2** (c = 1.5, T = 293 K)[a]

Compound	Conformer	Calculated specific OR (°)				Measured specific OR[a] (°)			
		589 nm	546 nm	436 nm	365 nm	589 nm	546 nm	436 nm	365 nm
1	**A**	−38	−47	−93	−181	**+36**	**+45**	**+91**	**+177**
	B	−23	−32	−58	−106				
ΔG Boltzmann averaged		**−38**	**−47**	**−93**	**−181**				
5	**A–A**	−36	−63	−126	−249				
	A–B	+213	+336	+645	+1215				
ΔG Boltzmann averaged		**+74**	**+113**	**+213**	**+395**				
***ent*-1**						**−38**	**−47**	**−93**	**−181**
2						**+40**	**+49**	**+91**	**+155**
***ent*-2**	**A**	−38	−63	−121	−223	**−39**	**−47**	**−87**	**−149**
	B	+37	+63	+133	+290				
ΔG Boltzmann averaged		**−32**	**−54**	**−103**	**−187**				
6	**A–A**	+32	+53	+109	+231				
	A–B	−121	−198	−384	−719				
	B–B	+99	+167	+342	+716				
ΔG Boltzmann averaged		**−8**	**−13**	**−20**	**−16**				

[a] Measured OR values were not normalized to 100% ee.

Computational analyses included (i) conformational analysis, (ii) geometry optimization of each low-energy conformer, (iii) calculation of the rotational strength and OR for individual stable conformers, and (iv) comparison between ΔG Boltzmann averaged calculated ECD spectra and calculated OR values with the experimental data.

DCCA may exist either as monomeric or as dimeric species whereby the equilibrium is likely to be strongly affected by the polarity of solvent. Dimerization may dramatically change the chiroptical properties of chiral molecules.[30] Therefore the computational study was carried out for **1** and ***ent*-2** as well as for dimeric forms **5** and **6**, which were derived from monomeric **1** and ***ent*-2**.

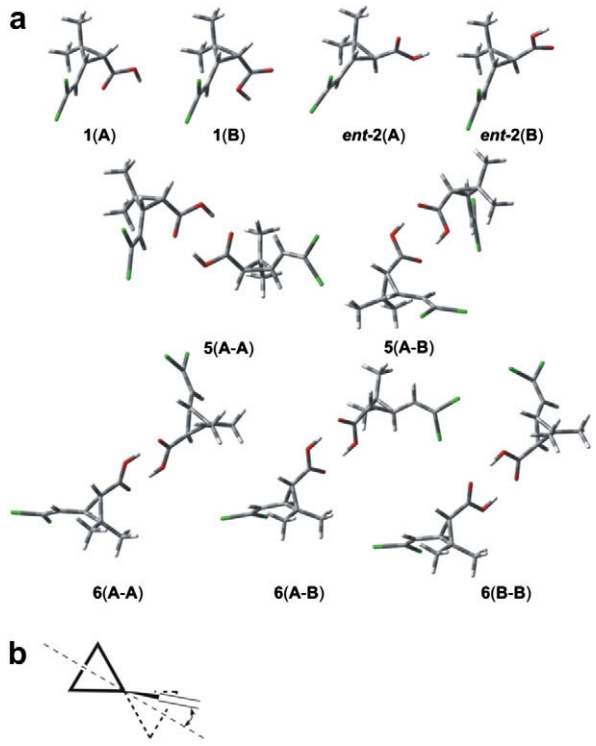

Figure 4. (a) Structures of individual conformers of monomeric **1** and ***ent*-2** and dimers **5** and **6** each calculated at the B3LYP/6-311++G(2D,2P) level. (b) Definition of acute angle between the cyclopropane bisector and the olefinic double bond. The transoid cyclopropane is drawn with bold lines, the cisoid with dashed lines.

Systematic conformational searches were performed taking absolute configurations of (1*R*,3*R*) for **1** and (1*S*,3*R*) for ***ent*-2**, respectively, as starting points (absolute configurations as derived from an X-ray crystallography study, vide supra). Due to the presence of the cyclopropane motif, DCCA is a relatively rigid molecule. Thus, its conformational dynamics are practically limited to the rotation of the gem-dichlorovinyl and the carboxylic acid group.

Conformational analysis of monomeric **1** and ***ent*-2** was carried out at the B3LYP/6-31G(D)//MM level followed by construction of the corresponding potential energy surface. Next, full structure optimizations at the B3LYP/6-311++G(2D,2P) level of theory were performed for the energy minima found on the potential energy surface. The results obtained for monomeric forms were used as input parameters in conformational analyses of dimers **5** and **6**, for which full structure optimizations at the B3LYP/6-311++G(2D,2P) level were also carried out. The final stage involved frequency calculations (B3LYP/6-311++G(2D,2P) level) for all optimized structures to confirm their stability. Percentage populations of conformers with relative energies of 0–2 kcal mol^{-1} were calculated for ΔG values using Boltzmann statistics (T = 298 K).

The structures of low-energy conformers of **1**, ***ent*-2**, **5**, and **6** are depicted in Figure 4.

As expected, only a small number of low-energy conformers were found. These conformers belong to two groups **A** and **B** which differ only in the orientation of the carboxylic group (**A** H–C*–C=O *anti*, **B** H–C*–C=O *syn*). For **1** a single conformer **A** was identified as the dominant one as the second conformer **B** is over 2 kcal mol^{-1} higher in energy (Table 3). On the other hand, ***ent*-2** can exist as one major **A** (93% abundance) and one minor **B** (7% abundance) conformer.

The calculated low-energy conformers of **1** and ***ent*-2** were used for construction of a set of possible dimers consisting of **A**–**A**, **A**–**B**, or **B**–**B** combinations. Common structural feature of **A**-type conformers is the *anti* conformation of the carboxylic group and the *syn* conformation of the vinyl substituent (defined correspondingly by H–C*–C=O and H–C–C=C angles). In contrast, the *syn* conformations of both the vinyl and the carboxylic substituents were found to be the less abundant **B**-type conformers. The corresponding values of acute angles between appropriate cyclopropane bisector and C=O or olefinic bonds ranged from −4.5° to +35° (Table 3). These structural features of monomeric species were consequently seen in the corresponding dimeric counterparts as well.

Both *anti* and *syn* conformations of carboxylic and gem-dichlorovinyl groups allowed for the interaction between degenerated Walsh orbitals of the cyclopropane ring and π-electrons of these

Table 3
Relative energies (ΔG) and populations as well as torsion (α, γ) and dihedral (β, δ) angles for low-energy conformers of **1**, ***ent*-2**, **5**, and **6** calculated at the B3LYP/6-311++G(2D,2P) level

Compound	Conformer	ΔG (kcal mol^{-1})	Population (%)	Angle (°)			
				α[a]	β[b]	γ[c]	δ[d]
1	**A**	0.00	100	174.7	−3.4	9.1	5.6
	B	2.48	—	−6.7	5.6	3.8	0.8
***ent*-2**	**A**	0.00	93	−167.7	10.0	2.9	2.5
	B	1.47	7	16.3	35.1	3.9	−0.6
5	**A**–**A**[e]	0.00	56	174.1	−4.5	8.6	4.8
	A–**B**	0.14	44	174.6, −6.2	−3.4, 5.0	7.3, 4.0	3.3, 0.3
6	**A**–**A**[e]	0.00	68	−168.4	9.3	5.5	0.2
	A–**B**	0.51	28	13.2, −168.1	32.0, 9.7	5.5, 4.6	0.8, 0.9
	B–**B**[e]	1.75	4	19.4	32.2	5.7	0.9

[a] α = H–C1–C=O.
[b] β = acute angle between cyclopropane bisector and C=O bond.
[c] γ = H–C3–C=C.
[d] δ = acute angle between bisector and C=C bond, for definition see Figure 4b.
[e] C_2 symmetry.

substituents.[45–47] The hydrogen bond formation between the carbonyl oxygen and the hydrogen atoms of the olefinic (**1**(**A**)) or one of the methyl ***ent*-2**(**A**) groups as well as a dipole–dipole interaction between the C=O and C*–H bonds can contribute further to stabilization of the respective conformers. Surprisingly, the dipole–dipole interaction between C=O and C*–H bonds does not seem to play a crucial role in the case of the monomeric conformers of DCCA. This is opposite to the dimers **5** and partially also **6** and stands also in contrast to the results obtained for tartaric acid and its derivatives.[48] For example, **5**(**A**–**B**) dimer is slightly less abundant than **5**(**A**–**A**), while the energy difference between the conformers of **5** is negligible. The lengths of hydrogen bonds connecting two monomeric moieties ranged from 1.677 Å to 1.702 Å, thus indicating strong bonding.

Oscillator and rotatory strengths (TDDFT/B3LYP/6-311++G(2D, 2P) level) and OR values (TDDFT/B3LYP/Aug-CC-pVDZ level) were calculated for thermally accessible conformers of **1**, ***ent*-2**, **5**, and **6**. Figure 5 depicts overlays of calculated (**1**, **5**, ***ent*-2**, and **6**) and measured (**1**, ***ent*-2**; both in acetonitrile) ECD spectra.

A reasonable overall agreement was found between the experimental and computed signs of Cotton effects. For **1** a very good reproduction was obtained with respect to both the positions of the Cotton effects and their relative amplitudes. For ***ent*-2** a less than perfect agreement was found which, however, still allowed unambiguous correlation of experimental and calculated short and long-wavelength Cotton effects. Calculated ECD spectra for the dimeric structures **5** and **6** were generally of higher amplitudes while the sign of the Cotton effect around 220 nm was in all cases positive and thus matched with experimental ECD data. Therefore the confrontation of measured and calculated ECD data conveniently allowed the unequivocal assignment of absolute configurations for DCCA stereoisomers and this assignment was fully in accordance with the data delivered by X-ray diffractometry (vide supra).

The origin of the Cotton effect of DCCA occurring at ca. 220 nm is the electronic transition involving mainly HOMO and LUMO orbitals (π–π^*), whereas transitions between HOMO and higher antibonding orbitals are responsible for the second shorter wavelength Cotton effect (Fig. 6).

The sign of the long-wavelength Cotton effect is, however, difficult to rationalize if only structural parameters of DCCA are consid-

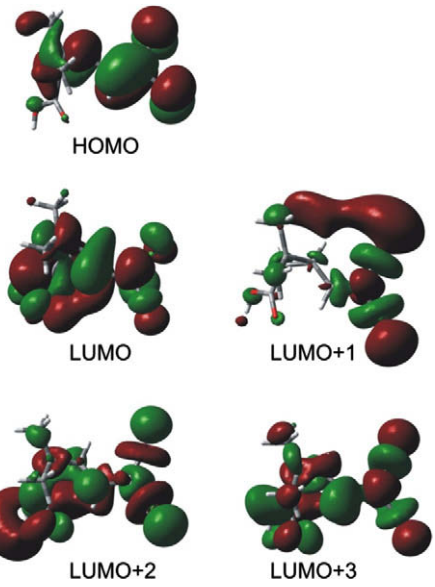

Figure 6. Molecular orbitals involved in the electronic transitions of **1**.

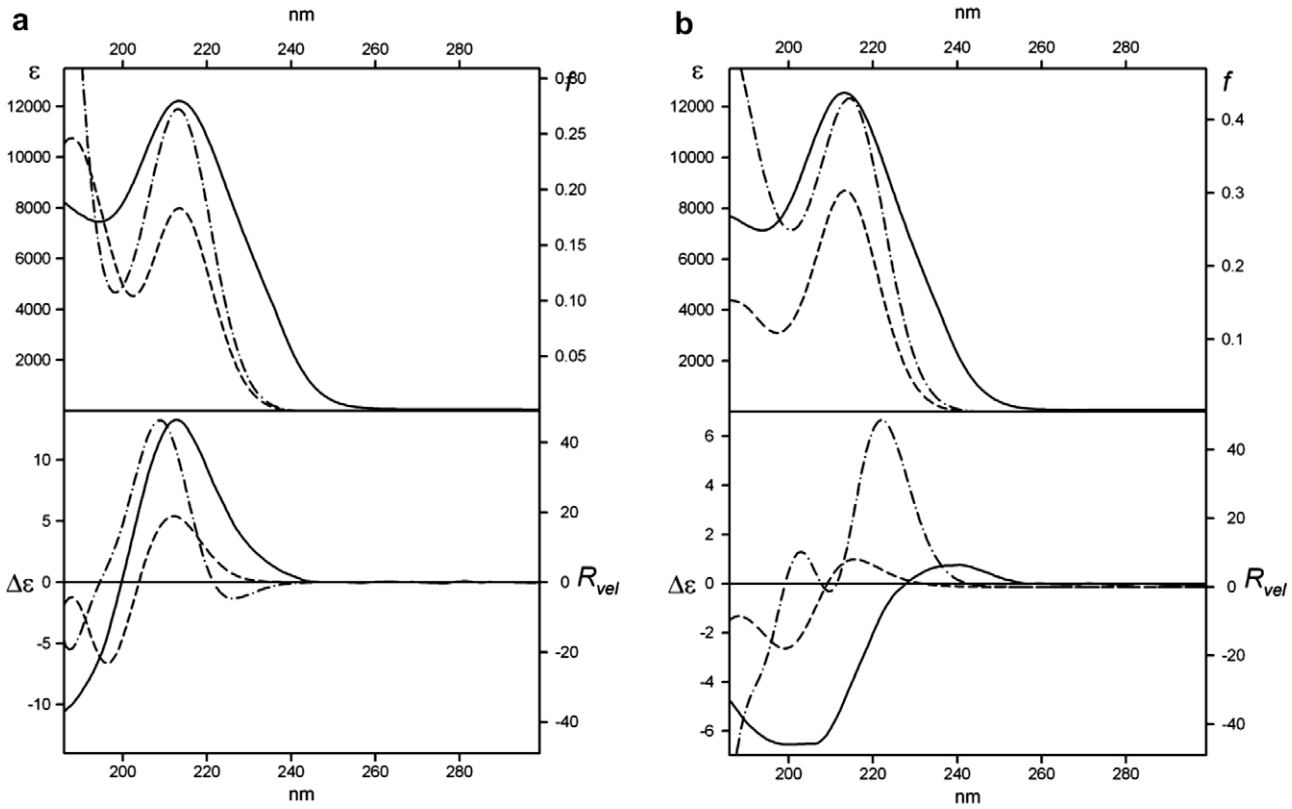

Figure 5. (a) Experimental (acetonitrile solution, solid lines, left column) and ΔG calculated Boltzmann averaged UV (upper panel) and ECD (lower panel) spectra of **1** (dashed lines, left column) and **5** (dash-dotted lines, left column). (b) Experimental (acetonitrile solution, solid lines, right column) and ΔG Boltzmann averaged UV (upper panel) and ECD (lower panel) spectra of ***ent*-2** (dashed lines, right column) and **6** (dash-dotted lines, right column). Calculations were performed at the TDDFT/B3LYP/6-311++G(2D,2P) level and spectra were wavelength corrected to match experimental long-wavelength λ_{max} values.

ered (Fig. 4b). For example, the acute angle between the bisector of the cyclopropane ring and the C=C bond of **1**(**A**) is positive, and the angle between the bisector and the C=O bond is negative while the situation is completely different for ***ent*-2**(**A**). Yet, in both cases the calculated rotatory strength for the π–π^* long-wavelength electronic transition is positive. Thus, the validity of the empirical rule proposed by Snatzke[41] needs further clarification.

Calculated OR values of DCCA stereoisomer ***ent*-2** and its dimer **6** well reproduced the experimental data and thus confirmed the assumed absolute configurations (Table 2). Regarding absolute OR values, the calculation for ***ent*-2** better reflected the experimental data. Possibly, the population of **6**(**A**–**B**), which is responsible for the net negative calculated ORs values for **6**, was simply underestimated. However, a disagreement between calculated and experimental OR data was found for monomeric enantiomer **1**. This may be due to the fact that in a non-polar environment (such as dichloromethane) monomer **1** predominantly exists as dimer **5**. ΔG Boltzmann averaged ORs of **5** calculated for the gas phase, are in accordance with the experimental data thus supporting this hypothesis.

3. Conclusions

The present approach to prepare PM stereoisomers in high ee via the DCCA intermediate can be extended to other pyrethroids as also cypermethrin and cyfluthrin contain the DCCA moiety. Further, the cinchona-type chiral stationary phases employed are capable of resolving stereoisomers of chrysanthemic acid and fenvaleric acid as well,[43] both of which are also pyrethroid synthons. This gives access to individual isomers of other pyrethroids by the same methodology. The individual PM stereoisomers prepared within this work were required for toxicological studies directed at the elucidation of stereoselectivity in the biological behavior of this widely used chiral insecticide.[44]

The chiroptical approach employed to determine absolute configurations via measured and calculated ECD and OR data was suitable for the stereochemical assignment of DCCA. Prerequisites are, however, a thorough conformational analysis and the consideration of (solvent-dependent) inter-molecular association which may influence the results considerably. The reliability of this confrontation approach was proven by reference data from X-ray crystallography.

Knowledge on the absolute configurations of DCCA allowed derivation of elution orders of DCCA stereoisomers on the employed Chiralpak QN-AX and Chiralpak QD-AX columns, thereby providing a chromatographic reference method for other studies. Under the conditions employed in Figure 3, the elution order on Chiralpak QN-AX was (1*R*,3*R*)-*cis*-DCCA < (1*R*,3*S*)-*trans*-DCCA < (1*S*,3*S*)-*cis*-DCCA < (1*S*,3*R*)-*trans*-DCCA. It is worth noting that the order of elution may be altered for the diastereomers upon a change of the elution conditions such as organic modifier type and content, pH or temperature. In particular the (1*R*,3*S*)-*trans*-DCCA and (1*S*,3*S*)-*cis*-DCCA isomers (middle peak pair) tend to co-elute under specific conditions or may even reverse their order of elution. In contrast, the enantiomer elution order was never found to be reversed under the elution conditions tested previously (polar organic and hydroorganic conditions with either methanol or acetonitrile as polar solvent and organic modifier, respectively).[43] On the other hand, the enantiomer elution order can conveniently be reversed by a switch to the corresponding Chiralpak QD-AX column, viz. (1*S*,3*S*)-*cis*-DCCA < (1*R*,3*R*)-*cis*-DCCA and (1*S*,3*R*)-*trans*-DCCA < (1*R*,3*S*)-*trans*-DCCA.[43]

Since the PM stereoisomers were obtained from DCCA stereoisomers by chemical transformation with preservation of the configurations, the absolute configurations of the synthesized individual PM stereoisomers could also be successfully assigned. Such unambiguous information on absolute configurations of biologically/toxicologically relevant chiral compounds (PM being a chiral pyrethroid-type pesticide, and DCCA being a mammalian phase I metabolite and environmental degradation product of PM) is central to the correct identification of stereoselectivity in fate and effect profiles and thus forms the basis for valid risk assessment.

4. Experimental

4.1. Chemicals

A *cis*/*trans*-DCCA stereoisomer mixture consisting of about 40% *cis*-DCCA and about 60% *trans*-DCCA was kindly provided by Agro-Chemie (Budapest, Hungary). Both oxalyl chloride and 3-phenoxybenzyl alcohol were supplied from Fluka (Buchs, Switzerland) in purum grade. Acetic acid (AcOH), dichloromethane (DCM) (both Fluka), *N*,*N*-dimethylformamide (Aldrich, Vienna, Austria), formic acid (Riedel de Haën, Seelze, Germany), 1-heptane (Fisher Scientific, Loughborough, UK), hydrochloric acid (Merck, Darmstadt, Germany), potassium hydroxide, *tert*-butyl methyl ether (TBME) (both Riedel de Haën), phosphoric acid (Merck), pyridine (Aldrich), sodium sulfate (Fluka), and triethyl amine (TEA) (Fluka) were of analytical grade. Acetonitrile (ACN), methanol (MeOH) (both Fisher Scientific), and water (Sigma–Aldrich) were of HPLC grade. For UV and ECD measurements acetonitrile, cyclohexane, and 1,2-dichloroethane of spectroscopic grade (all Aldrich) were used.

4.2. Instrumentation

Analytical HPLC runs were carried out on a HP1090 system from Agilent (Waldbronn, Germany) equipped with a diode array detector. Liquid chromatography in preparative scale was performed on a HPLC system from Bischoff Chromatography (Leonberg, Germany) (pump module: HPD pump multitherm 200 XL, UV-detector: Lambda 1010). ^{1}H NMR spectra were acquired on a Bruker DRX spectrometer with an operating frequency of 400 MHz (Bruker Optics, Vienna, Austria). For mass spectrometric measurements an API 365 triple–quadrupole system (Applied Biosystems, Thornhill, Canada) interfaced with a pneumatically assisted electrospray ionization source was used. OR values were determined with a polarimeter model 341 from Perkin Elmer (Vienna, Austria). UV and ECD spectra were recorded using a J-700 spectropolarimeter from Jasco Inc. (Easton, MD).

4.3. Preparation of DCCA stereoisomers

4.3.1. Diastereoselective preparative liquid chromatography of *cis*/*trans*-DCCA

A 50 mg mL^{-1} solution (1.0 mL) of *cis*/*trans*-DCCA in ACN/water/MeOH (50:50:0.1; v/v/v) was injected onto a 150 × 16 mm ID 10 μm Purospher Star RP-C18ec column (Merck, Darmstadt, Germany; packed by Austrian Research Centers, Seibersdorf, Austria) which was kept at 25 °C. Elution was carried out in isocratic mode at 10 mL min^{-1} with ACN/water/phosphoric acid (40:60:0.1; v/v/v) (detection wavelength 240 nm). After injection of total 2.5 g *cis*/*trans*-DCCA the combined fractions of each diastereomer (k^{trans} = 8.9; k^{cis} = 12.0) were concentrated at 35 °C under reduced pressure to remove ACN. The residual aqueous phases were extracted with 2 × 50 mL TBME. After drying the organic phase with sodium sulfate *cis*- and *trans*-DCCA were isolated by evaporation of the volatile fraction followed by drying at 10 mbar for 24 h at ambient temperature.

4.3.2. Enantioselective preparative liquid chromatography of *cis*- and *trans*-DCCA

cis- and *trans*-DCCA (each 0.55 g), respectively, prepared as reported above, was dissolved at a concentration of 100 mg mL^{-1} in ACN containing 20 mM AcOH and 2.5 mM TEA. This solution (0.5 mL) was injected onto a 250 × 20 mm ID 10 μm Chiralpak QD-AX column (Chiral Technologies Europe, Illkirch, France) which was kept at 25 °C. Isocratic elution was performed at 20 mL min^{-1} with 20 mM AcOH and 2.5 mM TEA in ACN (detection wavelength 240 nm). A crude product of each enantiomer (*cis*-DCCA: $k^{(1S,3S)}$ = 8.1, $k^{(1R,3R)}$ = 10.0; *trans*-DCCA: $k^{(1S,3R)}$ = 9.0, $k^{(1R,3S)}$ = 11.1) was obtained after evaporation of the volatile fraction. Treatment with 30 mL of 1% aqueous phosphoric acid, extraction with 2 × 25 mL 1-heptane, and evaporation of the latter phase afforded the individual DCCA stereoisomers as white crystals, which were finally dried at 10 mbar for 24 h at ambient temperature.

***cis*-DCCA**: ^{1}H NMR (400 MHz, $CDCl_3$): 6.21 (d, 1H), 2.10 (t, 1H), 1.85 (d, 1H), 1.28 (s, 3H), 1.27 (s, 3H) ppm; ESI-MS: 207.0 [M−H]$^-$; ***trans*-DCCA**: ^{1}H NMR (400 MHz, $CDCl_3$): 5.62 (d, 1H), 2.27 (dd, 1H), 1.62 (d, 1H), 1.33 (s, 3H), 1.21 (s, 3H) ppm; ESI-MS: 207.0 [M−H]$^-$; **(1*R*,3*R*)-*cis*-DCCA 1**: 99.1% diast. purity, 99.8% ee, $[\alpha]^{20}_{365}$ = +176.6, $[\alpha]^{20}_{436}$ = +90.7, $[\alpha]^{20}_{546}$ = +45.3, $[\alpha]^{20}_{589}$ = +36.5 (*c* 1.5, DCM); **(1*S*,3*S*)-*cis*-DCCA *ent*-1**: 99.1% diast. purity, 99.2% ee, $[\alpha]^{20}_{365}$ = −181.3, $[\alpha]^{20}_{436}$ = −93.1, $[\alpha]^{20}_{546}$ = −46.6, $[\alpha]^{20}_{589}$ = −38.0 (*c* 1.5, DCM); **(1*R*,3*S*)-*trans*-DCCA 2**: >99.95% diast. purity, 99.2% ee, $[\alpha]^{20}_{365}$ = +154.7, $[\alpha]^{20}_{436}$ = +90.6, $[\alpha]^{20}_{546}$ = +49.2, $[\alpha]^{20}_{589}$ = +40.3 (*c* 1.5, DCM); **(1*S*,3*R*)-*trans*-DCCA *ent*-2**: >99.95% diast. purity, 99.8% ee, $[\alpha]^{20}_{365}$ = −148.7, $[\alpha]^{20}_{436}$ = −86.9, $[\alpha]^{20}_{546}$ = −47.0, $[\alpha]^{20}_{589}$ = −38.8 (*c* 1.5, DCM).

4.4. Preparation of PM stereoisomers

At first, 150 mg (0.72 mmol) of the respective chromatographically purified DCCA stereoisomer was dissolved in 5 mL DCM. After addition of 150 μL oxalyl chloride (2.16 mmol) the reaction mixture was stirred at 25 °C for 2 h under nitrogen. Then 10 μL *N*,*N*-dimethylformamide was added and stirring was continued for further 14 h. The volatile fraction was then carefully removed by evaporation and dried for 1 h at 40 °C and 10 mbar. The remaining oil was dissolved in 8 mL DCM followed by the addition of 250 μL 3-phenoxybenzyl alcohol (1.43 mmol) and 65 μL (0.80 mmol) pyridine. The mixture was stirred at ambient temperature and anhydrous conditions for 6 h. After evaporation the residual product was treated with 2 × 5 mL TBME and the precipitated pyridine chloride salt was removed by filtration. The volatile fraction was evaporated and the residual oil was dissolved in 7.5 mL ACN/water/phosphoric acid (80:20:0.1; v/v/v). Chromatographic purification was carried out by injecting 1.5 mL fractions onto the preparative Purospher Star RP-C18ec column (vide supra) and isocratic elution at 10 mL min^{-1} with ACN/water/phosphoric acid (80:20:0.1; v/v/v) (detection wavelength 230 nm). The organic modifier of the collected and combined PM peak fraction was evaporated and the oily layer of the remaining aqueous phase was extracted with 2 × 25 mL TBME. After drying with sodium sulfate and evaporation each PM stereoisomer was obtained as colorless oil. Drying at 10 mbar for 24 h at ambient temperature afforded *cis*-PM enantiomers as white crystals whereas *trans*-PM enantiomers remained oily. PM stereoisomers were stored at −20 °C until further use.

***cis*-PM**: ^{1}H NMR (400 MHz, $CDCl_3$): 7.38–6.93 (m, 9H), 6.26 (d, 1H), 5.08 (s, 2H), 2.03 (t, 1H), 1.89 (d, 1H), 1.24 (s, 3H), 1.23 (s, 3H) ppm; ESI-MS: 391.1 [M+H]$^+$; ***trans*-PM**: ^{1}H NMR (400 MHz, $CDCl_3$): 7.38–6.94 (m, 9H), 5.60 (d, 1H), 5.10 (s, 2H), 2.26 (dd, 1H), 1.65 (d, 1H), 1.27 (s, 3H), 1.18 (s, 3H) ppm; ESI-MS: 391.1 [M+H]$^+$; **(1*R*,3*R*)-*cis*-PM 3**: 65% yield; >99.95% diast. purity, 99.7% ee, $[\alpha]^{20}_{365}$ = +19.7, $[\alpha]^{20}_{436}$ = +8.5, $[\alpha]^{20}_{546}$ = +3.7, $[\alpha]^{20}_{589}$ = +2.6 (*c* 1.5, DCM); **(1*S*,3*S*)-*cis*-PM *ent*-3**: 70% yield; >99.95% diast. purity, 99.6% ee, $[\alpha]^{20}_{365}$ = −22.5, $[\alpha]^{20}_{436}$ = −10.4, $[\alpha]^{20}_{546}$ = −4.6, $[\alpha]^{20}_{589}$ = −3.7 (*c* 1.5, DCM); **(1*R*,3*S*)-*trans*-PM 4**: 63% yield; 99.94% diast. purity, 99.3% ee, $[\alpha]^{20}_{365}$ = −45.3, $[\alpha]^{20}_{436}$ = −20.5, $[\alpha]^{20}_{546}$ = −9.6, $[\alpha]^{20}_{589}$ = −8.0 (*c* 1.5, DCM); **(1*S*,3*R*)-*trans*-PM *ent*-4**: 69% yield; >99.95% diast. purity, 99.8% ee, $[\alpha]^{20}_{365}$ = +46.7, $[\alpha]^{20}_{436}$ = +21.3, $[\alpha]^{20}_{546}$ = +10.3, $[\alpha]^{20}_{589}$ = +8.4 (*c* 1.5, DCM).

4.5. Chromatographic purity assessment

Each of the four stereoisomers of DCCA and PM were checked chromatographically for chemical and diastereomer purity with a 150 × 4.6 mm ID 10 μm Purospher Star RP18ec (Merck) column. For DCCA isocratic elution was performed at 25 °C and 1.0 mL min^{-1} with ACN/water/phosphoric acid (40:60:0.1; v/v/v), while PM was analyzed with ACN/water/phosphoric acid (80:20:0.1; v/v/v) under otherwise identical conditions. Then 10 μL of a 2 mg mL^{-1} solution of DCCA and a 4 mg mL^{-1} solution of PM, respectively, were injected and peak monitoring was carried out at 230 nm.

Determination of ee of DCCA stereoisomers was performed by stereoselective liquid chromatography with a 150 × 4 mm ID 5 μm Chiralpak QN-AX (Chiral Technologies Europe) column. The flow rate was adjusted to 0.8 mL min^{-1} and stereoselective separation was carried out with ACN/MeOH/AcOH (95:5:0.1; v/v/v) at 25 °C (detection wavelength: 230 nm). Then, 10 μL of a 2 mg mL^{-1} solution of the individual DCCA stereoisomers was injected.

To confirm the absence of racemization in the course of esterification, 2 mg of each PM stereoisomer was dissolved in 200 μL ACN. Aqueous potassium hydroxide solution (500 μL 2 M) was added and quantitative hydrolysis was yielded by incubating the reaction mixture at 40 °C for 24 h. Afterwards, the ACN was removed with a gentle stream of nitrogen and DCCA was obtained by extraction of the acidified aqueous phase (addition of 100 μL concentrated hydrochloric acid) with 500 μL TBME. After removal of the volatile fraction with a gentle stream of nitrogen the residual DCCA was analyzed by stereoselective HPLC under the above specified conditions for DCCA ee determination using Chiralpak QN-AX.

4.6. X-ray crystallography

All four single DCCA stereoisomers were co-crystallized with *O*-9-(2,6-diisopropylphenylcarbamoyl)quinine in chloroform/1-heptane. Detailed experimental information on the diffractometric analysis is given in an earlier communication.[42] Crystallographic data (excluding structure factors) for the structures have been deposited with the Cambridge Crystallographic Data Centre as Supplementary Publication Numbers CCDC 665833–665836. Copies of the data can be obtained, free of charge, on application to CCDC, 12 Union Road, Cambridge CB2 1EZ, UK [fax: +44(0)-1223-336033 or e-mail: deposit@ccdc.cam.ac.uk].

4.7. UV and ECD spectroscopy

All measurements were carried out at an optical pathlength of 1 mm and concentration values of ca. 9 × 10^{-4} M (DCCA) and ca. 3 × 10^{-4} M (PM), respectively. Spectral conditions were as follows: bandwidth 0.5 nm, scan speed 100 nm min^{-1}, response time 1 s. Acetonitrile (λ^{min} = 185 nm) and cyclohexane containing 5% (v/v) 1,2-dichloroethane (λ^{min} = 200 nm) were employed as solvents. All spectra were corrected using the respective blank solvents. Absorption and ECD spectra were simultaneously reprocessed using the methodology of Arvinte.[49]

4.8. Computational details

Initial conformational analyses of **1** and ***ent*-2** were performed by MM3 force field (CaChe Conflex software, Fujitsu Ltd, Tokyo, Japan. Fifty four conformations for **1** and 63 conformations for ***ent*-2** were obtained, which were optimized using B3LYP hybrid functional and a 6-31g(d) basis set (GAUSSIAN 03[50]). The conformers with relative energies between 0 and 5 kcal mol^{-1} were refined using the same hybrid functional and the enhanced basis set 6-311++G(2D,2P). Finally, for these structures frequency calculations were carried out at the B3LYP/6-311++G(2D,2P) level of theory to establish their stability. For conformers having the relative energy ranging from 0 to 2 kcal mol^{-1} percentage populations were calculated on the basis of ΔE and ΔG values, using Boltzmann statistics and $T = 298$ K. Due to their similarity only ΔG values were taken into further considerations.

Excited-state calculations of **1** and ***ent*-2** using TDDFT (GAUSSIAN 03[50]) were based on the ground state geometries of single molecules. Calculations of oscillator and rotatory strengths were performed at the B3LYP/6-311++G(2D,2P) level of theory. Rotatory strengths were calculated using both length and velocity representations. Due to minor differences between the length and velocity of calculated values of rotatory strengths only velocity representations were taken into account. ECD spectra were simulated by overlapping Gaussian functions for each transition according to the procedure described previously.[12] Specific OR values at 365, 436, 546, and 589 nm were calculated at the B3LYP/Aug-CC-pVDZ level of theory.

Additionally, using the same methodology as described above, structures as well as chiroptical properties of dimeric forms **5** and **6** were calculated. The possible structures of dimers were constructed with the use of fully optimized structures of the corresponding monomeric species.

Acknowledgments

The financial support by the Austrian Christian Doppler Research Society and the industry partners Merck KGaA (Darmstadt, Germany), AstraZeneca (Mölndal, Sweden), and Sandoz (Kundl, Austria) is gratefully acknowledged. Part of this work was supported by a Grant No. N N204 056335 from the Ministry of Science and Higher Education (to M.K.). All calculations were performed at Poznań Supercomputing Center, Poland.

References

1. Flack, H. D.; Bernardinelli, G. *Chirality* **2008**, *20*, 681–690.
2. Ladd, M. F. C.; Palmer, R. A. *Structure Determination by X-ray Crystallography*, 2nd ed.; Plenum Press: New York, 1985.
3. Berova, N.; Nakanishi, K.; Woody, R. W. *Circular Dichroism: Principles and Applications*, 2nd ed.; Wiley-VCH: New York, 2000.
4. Crawford, T. D.; Stephens, P. J. *J. Phys. Chem. A* **2008**, *112*, 1339–1345.
5. Dierksen, M.; Grimme, S. *J. Chem. Phys.* **2006**, *124*, 174301/1–174301/12.
6. Mori, T.; Inoue, Y.; Grimme, S. *J. Org. Chem.* **2006**, *71*, 9797–9806.
7. Burke, K.; Werschnik, J.; Gross, E. K. U. *J. Chem. Phys.* **2005**, *123*, 062206/1–062206/9.
8. Gawronski, J.; Kwit, M.; Boyd, D. R.; Drake, A.; Malone, J. F.; Sharma, N. D. *J. Am. Chem. Soc.* **2005**, *127*, 4308–4319.
9. Marchesan, D.; Coriani, S.; Forzato, C.; Nitti, P.; Pitacco, G.; Ruud, K. *J. Phys. Chem. A* **2005**, *109*, 1449–1453.
10. Lattanzi, A.; Viglione, R. G.; Scettri, A.; Zanasi, R. *J. Phys. Chem. A* **2004**, *108*, 10749–10753.
11. McCann, D. M.; Stephens, P. J.; Cheeseman, J. R. *J. Org. Chem.* **2004**, *69*, 8709–8717.
12. Diedrich, C.; Grimme, S. *J. Phys. Chem. A* **2003**, *107*, 2524–2539.
13. Ruud, K.; Stephens, P. J.; Devlin, F. J.; Taylor, P. R.; Cheeseman, J. R.; Frisch, M. J. *Chem. Phys. Lett.* **2003**, *373*, 606–614.
14. Stephens, P. J.; Devlin, F. J.; Cheeseman, J. R.; Frisch, M. J.; Bortolini, O.; Besse, P. *Chirality* **2003**, *15*, S57–S64.
15. Autschbach, J.; Ziegler, T.; van Gisbergen, S. J. A.; Baerends, E. J. *J. Chem. Phys.* **2002**, *116*, 6930–6940.
16. Grimme, S. *Chem. Phys. Lett.* **2001**, *339*, 380–388.
17. Stephens, P. J.; Devlin, F. J.; Cheeseman, J. R.; Frisch, M. J. *J. Phys. Chem. A* **2001**, *105*, 5356–5371.
18. Zhao, Y.; Truhlar, D. G. *Acc. Chem. Res.* **2008**, *41*, 157–167.
19. Kwit, M.; Sharma, N. D.; Boyd, D. R.; Gawronski, J. *Chirality* **2008**, *20*, 609–620.
20. Kwit, M.; Sharma, N. D.; Boyd, D. R.; Gawronski, J. *Chem. Eur. J.* **2007**, *13*, 5812–5821.
21. Kundrat, M. D.; Autschbach, J. *J. Phys. Chem. A* **2006**, *110*, 4115–4123.
22. Kundrat, M. D.; Autschbach, J. *J. Phys. Chem. A* **2006**, *110*, 12908–12917.
23. Pecul, M. *Chem. Phys. Lett.* **2006**, *418*, 1–10.
24. Pecul, M.; Ruud, K.; Rizzo, A.; Helgaker, T. *J. Phys. Chem. A* **2004**, *108*, 4269–4276.
25. Wiberg, K. B.; Vaccaro, P. H.; Cheeseman, J. R. *J. Am. Chem. Soc.* **2003**, *125*, 1888–1896.
26. Specht, K. M.; Nam, J.; Ho, D. M.; Berova, N.; Kondru, R. K.; Beratan, D. N.; Wipf, P., ; Pascal, R. A., Jr.; Kahne, D. *J. Am. Chem. Soc.* **2001**, *123*, 8961–8966.
27. Stephens, P. J.; McCann, D. M.; Devlin, F. J.; Smith, A. B., III *J. Nat. Prod.* **2006**, *69*, 1055–1064.
28. Stephens, P. J.; McCann, D. M.; Butkus, E.; Stončius, S.; Cheeseman, J. R.; Frisch, M. J. *J. Org. Chem.* **2004**, *69*, 1948–1958.
29. Stephens, P. J.; McCann, D. M.; Devlin, F. J.; Cheeseman, J. R.; Frisch, M. J. *J. Am. Chem. Soc.* **2004**, *126*, 7514–7521.
30. Wang, F.; Polavarapu, P. L.; Drabowicz, J.; Kiełbasiński, P.; Potrzebowski, M. J.; Mikołajczyk, M.; Wieczorek, M. W.; Majzner, W. W.; Łazowska, I. *J. Phys. Chem. A* **2004**, *108*, 2072–2079.
31. Chamberlain, K.; Matsuo, N.; Kaneko, H.; Khambay, B. P. S. In *Pyrethroids*; Kurihara, N., Miyamoto, J., Eds.; Chirality in Agrochemicals; John Wiley & Sons: Chichester, 1998; pp 9–84.
32. Rauk, A. *Orbital Interaction Theory of Organic Chemistry*, 2nd ed.; John Wiley & Sons: New York, 2001.
33. Craig, J. C.; Kollman, P. A.; Lee, S. Y. C.; Moore, R. E.; Pettus, J. A., Jr.; Rothenberg, S. *J. Chem. Soc., Perkin Trans. 2* **1978**, 1338–1344.
34. Heathcock, C. H.; Poulter, S. R. *J. Am. Chem. Soc.* **1968**, *90*, 3766–3769.
35. Skepper, C. K.; MacMillan, J. B.; Zhou, G. X.; Masuno, M. N.; Molinski, T. F. *J. Am. Chem. Soc.* **2007**, *129*, 4150–4151.
36. Crombie, L.; Findlay, D. A. R.; King, R. W.; Shirley, I. M.; Whiting, D. A.; Scopes, P. M.; Tracey, B. M. *Chem. Commun.* **1976**, *12*, 474–475.
37. Begley, M. J.; Crombie, L.; Simmonds, D. J.; Whiting, D. A. *J. Chem. Soc., Perkin Trans. 1* **1974**, *11*, 1230–1235.
38. Sasaki, T.; Eguchi, S.; Ohno, M. *J. Org. Chem.* **1972**, *37*, 466–469.
39. Jorgenson, M. J.; Leung, T. *J. Am. Chem. Soc.* **1968**, *90*, 3769–3774.
40. Połoński, T.; Milewska, M. J.; Katrusiak, A. *J. Org. Chem.* **1993**, *58*, 3411–3415.
41. Snatzke, G. *Pure Appl. Chem.* **1979**, *51*, 769–785.
42. Bicker, W.; Chiorescu, I.; Arion, V. B.; Lämmerhofer, M.; Lindner, W. *Tetrahedron: Asymmetry* **2008**, *19*, 97–110.
43. Bicker, W.; Lämmerhofer, M.; Lindner, W. *J. Chromatogr., A* **2004**, *1035*, 37–46.
44. Dornetshuber, J.; Bicker, W.; Staniek, K.; Lämmerhofer, M; Lindner, W.; Karwan, A.; Bursch, W., in preparation.
45. Wiberg, K. B. *Acc. Chem. Res.* **1996**, *29*, 229–234.
46. Hoffman, R.; Heilbronner, E.; Gleiter, R. *J. Am. Chem. Soc.* **1970**, *92*, 706–707.
47. Walsh, A. D. *Nature* **1947**, *159*, 165.
48. Rychlewska, U.; Wascinska, N.; Warżajtis, B.; Gawronski, J. *Acta Crystallogr., Sect. B* **2008**, *64*, 497–503.
49. Arvinte, T.; Bui, T. T. T.; Dahab, A. A.; Demeule, B.; Drake, A. F.; Elhag, D.; King, P. *Anal. Biochem.* **2004**, *332*, 46–57.
50. Frisch, M. J.; Trucks, G. W.; Schlegel, H. B.; Scuseria, G. E.; Robb, M. A.; Cheeseman, J. R.; Montgomery, J. A., Jr.; Vreven, T.; Kudin, J. A.; Burant, J. C.; Millam, J. M.; Iyengar, S. S.; Tomasi, J.; Barone, V.; Mennucci, B.; Cossi, M.; Scalmani, G.; Rega, N.; Petersson, G. A.; Nakatsuji, H.; Hada, M.; Ehara, M.; Toyota, K.; Fukuda, R.; Hasegawa, J.; Ishida, M.; Nakajima, T.; Honda, Y.; Kitao, O.; Nakai, H.; Klene, M.; Li, X.; Knox, J. E.; Hratchian, H. P.; Cross, J. B.; Bakken, V.; Adamo, C.; Jaramillo, J.; Gomperts, R.; Stratmann, R. E.; Yazyev, O.; Austin, A. J.; Cammi, R.; Pomelli, C.; Ochterski, J. W.; Ayala, P. Y.; Morokuma, K.; Voth, G. A.; Salvador, P.; Dannenberg, J. J.; Zakrzewski, V. G.; Dapprich, S.; Daniels, A. D.; Strain, M. C.; Farkas, O.; Malick, D. K.; Rabuck, A. D.; Raghavachari, K.; Foresman, J. B.; Ortiz, J. V.; Cui, Q.; Baboul, A. G.; Clifford, S.; Cioslowski, J.; Stefanov, B. B.; Liu, G.; Liashenko, A.; Piskorz, P.; Komaromi, I.; Martin, R. L.; Fox, D. J.; Keith, T.; Al-Laham, M. A.; Peng, C. Y.; Nanayakkara, A.; Challacombe, M.; Gill, P. M. W.; Johnson, B.; Chen, W.; Wong, M. W.; Gonzalez, C.; Pople, J. A. *GAUSSIAN 03, Revision D.01*, Gaussian: Wallingford, CT, 2004.